

Functional and structural determinants of reverse operation in the pH-dependent oligopeptide transporter PepT1

Maria Daniela Renna · Ayodele Stephen Oyadeyi ·
Elena Bossi · Gabor Kottra · Antonio Peres

Received: 22 July 2010/Revised: 20 October 2010/Accepted: 25 November 2010/Published online: 23 December 2010
© Springer Basel AG 2010

Abstract The functional and structural basis of reverse operation of PepT1 has been studied in *Xenopus* oocytes expressing the wild-type and mutated forms of this protein. Using brief pulses from a negative holding potential, wild-type and Arg282 mutants exhibit outward currents in the presence of Gly-Gln. The reversal potential of these currents is affected by both pH and substrate concentration, confirming coupled transport in the wild type and in the mutants as well. Long-lasting voltage and current-clamp experiments show that the outward currents are only temporary, and reflect accumulation and/or depletion effects near the membrane. The ability to operate in reverse mode was confirmed in all isoforms by intracellular injection of substrate. The role of Arg282 and Asp341 in the reverse transport was also investigated using charged substrates. Positive Lys-Gly (but not Gly-Lys) showed enhanced transport currents in the Arg282 mutants. In contrast, negative Gly-Asp and Asp-Gly elicited modest currents in all isoforms.

Keywords Transporter · Reverse operation · Structure-function · Electrophysiology · *Xenopus* oocyte · PepT1

Introduction

The main function of the intestinal peptide transporter PepT1 (SLC15 family) is the efficient and energy-saving absorption of small peptides originating from food proteins. This process is driven by the cotransport of protons and thus generates an inwardly directed current. However, under certain experimental conditions outward currents have been observed in the zebrafish isoform of PepT1 [1] and also in a mammalian isoform [2]. Interestingly, in this last case it was reported that the outward currents were greatly enhanced in conditions of high intracellular substrate concentration or following inhibition of intracellular dipeptide hydrolysis. Furthermore, the renal isoform of the peptide transporter, PepT2, has been identified among others in the enteric nervous system in both glia cells, and a specific subset of neurons and could play a role in both release and reabsorption of small neuropeptides [3].

The question of reverse operation is a relevant issue in many cotransport systems, especially in the context of neurological disorders in which leakage of neurotransmitters into the extracellular space may have profound consequences. Although the physiological role of these transporters is the reuptake, in several instances a release of neurotransmitter via the transporter has been reported. This reversed mode of operation may be either the effect or the cause of abnormal or pathological conditions. In the case of the glutamate transporters, export of glutamate may lead to the elevated extracellular levels that cause excitotoxicity [4], while in the SLC6 family reversal of the operation of

M. D. Renna and A. S. Oyadeyi contributed equally.

M. D. Renna · A. S. Oyadeyi · E. Bossi · A. Peres (✉)
Laboratory of Cellular and Molecular Physiology,
Dept. of Biotechnology and Molecular Sciences,
University of Insubria, Via Dunant 3, 21100 Varese, Italy
e-mail: antonio.peres@uninsubria.it

E. Bossi · A. Peres
Center for Neurosciences, University of Insubria,
21100 Varese, Italy

G. Kottra
Molecular Nutrition Unit,
Technische Universität München, Freising, Germany

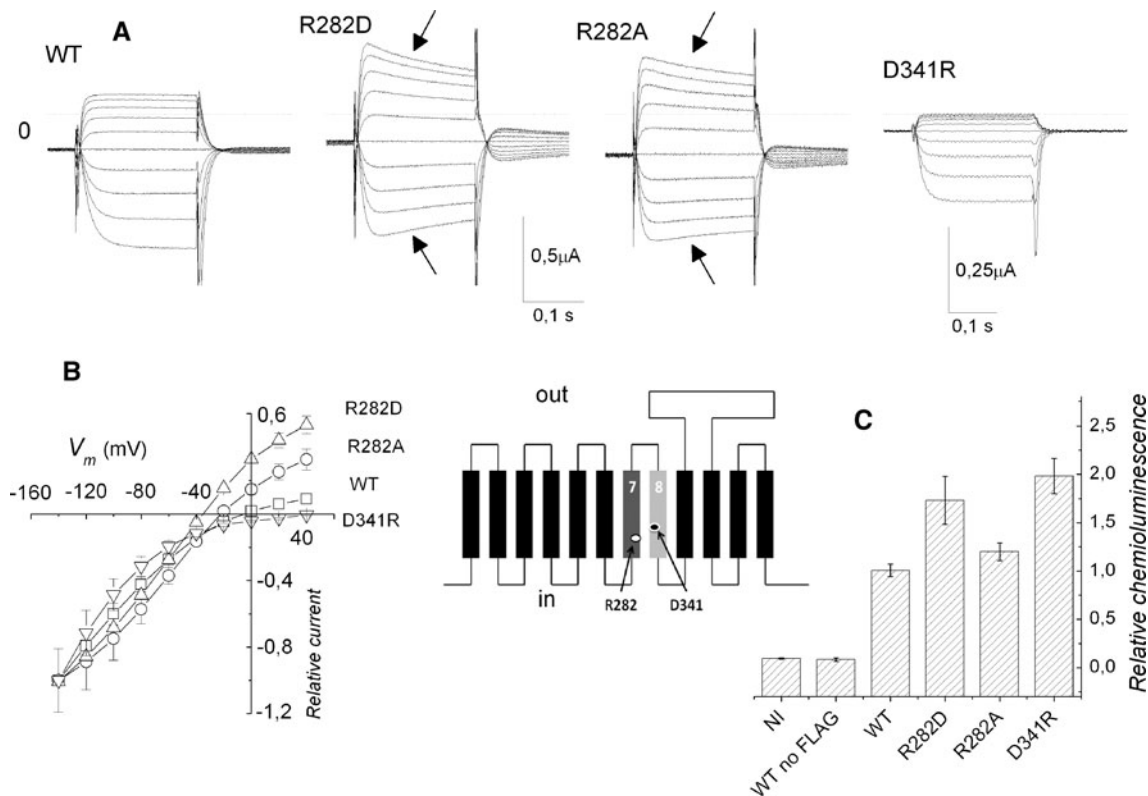


Fig. 1 **A** Representative transport currents recorded in the wild-type and indicated mutants in the presence of 1 mM Gly-Gln at pH 8.0. Voltage pulses from -140 to $+40$ mV were applied from $V_h = -60$ mV. The dotted lines indicate the zero-current level and the arrows the declining behavior of the currents. Note the amplified scale for the D341R mutant. **B** I/V relationships, averaged after normalization for each oocyte to the current at -140 mV (mean \pm SE,

$n = 4-7$ from two batches). **C** Surface expression, reported as results of the chemiluminescence experiments from oocytes expressing the wild-type and the indicated mutants of PepT1-FLAG. The chemiluminescence detected from 20 to 40 oocytes from three different batches secondarily labeled with peroxidase-conjugated goat anti-mouse, IgG-HRP are shown. The data were normalized to the mean value of the wild-type FLAG-PepT1 of each batch

the dopamine transporter is caused by amphetamines [5] [6], and release of GABA through GAT1 has been hypothesized to concur in causing epileptic seizures [7, 8].

Although the SLC15 family is distinct from the gene families of the neurotransmitter transporters cited above (SLC1 and SLC6), there is growing evidence that different families may share common structural modules [9–11]. It is conceivable therefore that an investigation of the structural determinants of reverse operation in PepT1 may contribute to understanding the same process in the neurotransmitter transporters.

Mutations of single amino acids may result in considerable changes of the transport function of nutrient transporters. In the case of PepT1, the conserved residue histidine 57, predicted to reside in the second transmembrane segment, and the corresponding residue His 87 in PepT2 were found to be essential for the functioning, whereas tyrosine residues adjacent to H57 seem to stabilize the cotransported proton when interacting with H57 [12, 13]. The nearby histidine residue His 121 (and His 142 in PepT2) is not essential, but influences the substrate

binding, as H121 mutants have shown decreased affinities [14]. The tyrosine residue Y167 has an important function as well, since its mutation to alanine completely abolished transport via PepT1 [15]. By using the cysteine scanning method, Kulkarni and coworkers [16] identified several residues important for the transport function in transmembrane segments 5 and 7 and suggested that these segments line the putative aqueous channel. Finally, the same authors identified two oppositely charged residues (R282 and D341) in transmembrane segments 7 and 8, respectively, that form a salt bridge and play an important role in the substrate translocation via PepT1 [17].

We have recently observed (unpublished observations) that two rbPepT1 mutants in arginine 282 (R282D and R282A) exhibit large outward transport currents that remain pH- and substrate concentration-dependent. Arginine 282 is located in the seventh transmembrane segment of the protein, and it is believed to form a charge pair with another, negatively charged residue (aspartate 341), positioned at about the same level in transmembrane segment 8 (see inset in Fig. 1) [9, 17, 18].

An analogous mutant (R282E) of rabbit PepT1 was previously reported to exhibit characteristics similar to a substrate-gated unspecific cation channel [19]. In this paper we therefore investigated the properties of reverse operation in the R282D and R282A mutants to understand to what degree the operation of PepT1 was modified from a coupled-transport mode to a channel mode, obeying the principles of electrodiffusion.

The hypothesis of an important role of local accumulation/depletion of substrate near the intra- and extracellular sides of the transporter, which has been previously suggested [20], was tested by employing different experimental protocols aimed at altering the transport regime by long-lasting holding potentials.

PepT1 transporters show relatively poor substrate specificity [21]: many di- and tri-peptides, either neutral or electrically charged, are transported, while single amino acids and tetrapeptides are not [22, 23]. Having observed enhanced outward currents in mutants in which the positive R282 was removed, the importance of a charge in the substrate was also investigated, using both positively and negatively charged dipeptides, in addition to the zwitterionic Gly-Gln.

Materials and methods

Construction of point mutations

Mutations in rabbit PepT1 were obtained by site-directed mutagenesis (Quickchange Site-Directed Mutagenesis Kit, Stratagene Inc., Milan, Italy). Briefly, 20 ng of the plasmid containing the FLAG-wild-type PepT1 cDNA [24] was amplified with 2.5 units of *Pfu* DNA polymerase in the presence of overlapping primers containing in their sequence the mutated codons:

rbPepT1 R282D: 5'-CGCGCAGATCAAGATGGTTACG
GATGTGCTGTTCTGTACATCCC-3'

rbPepT1 R282A: 5'-CGCGCAGATCAAGATGGTTACG
GCGGTGCTGTTCTGTACATCCC-3'

rbPepT1 D341R: 5'-CCTGGTCCCCATCATGCGCGCC
GTGGTGTATCC-3'

PCR amplification was performed with 25 thermal cycles of 95°C for 30 s, 55°C for 1 min, and 68°C for 14 min. Then, 10 units of *DpnI* was added directly to the amplification reaction, and the sample was incubated for 1 h at 37°C to digest the parental, methylated DNA. JM109 supercompetent cells were finally transformed with 1 µl of the reaction mixture and plated onto LB-ampicillin plates. After plasmid purification, plasmid cDNAs were fully sequenced (Eurofin MWG Operon Biotech).

Oocyte expression

Oocytes and RNAs were prepared as described in detail previously [25]. In summary, to prepare the mRNA, the cDNA encoding PepT1-FLAG transporters, cloned into the pSPORT-1 vector [24], were linearized with NotI; subsequently cRNA was synthesized in vitro in the presence of Cap Analog and 200 units of T7 RNA polymerase. All enzymes were supplied by Promega Italia, Milan, Italy. Oocytes were obtained from adult female *Xenopus laevis*, the frogs were anesthetized in MS222 (tricaine methanesulfonate) 0.10%(w/v) solution in tap water, and portions of the ovary were removed through an incision on the abdomen. The oocytes were treated with collagenase (Sigma Type IA) 1 mg/ml in ND96 Ca⁺ free for at least 1 h at 18°C. After 24 h at 18°C in modified Barth's saline solution (MBS), the healthy looking oocytes were injected with 12.5 ng of cRNA in 50 nl of water, using a manual microinjection system (Drummond). The oocytes were then incubated at 18°C for 3–4 days in MBS before electrophysiological studies. The experiments were carried out according to the institutional and national ethics guidelines (permit no. 12/09).

Single-oocyte chemiluminescence

The expression of PepT1-FLAG isoforms at the oocyte plasma membrane was determined by the single oocyte chemiluminescence (SOC) technique [26–28], which employs enzyme amplification with a chemiluminescent substrate and sensitive linear detection with a luminometer. Oocytes expressing different FLAG-PepT1 isoforms, as well as non-transfected oocytes, were washed twice for 5 min in ice-cold ND96 pH 7.6 and then fixed with 4% paraformaldehyde in ND96 for 15 min at 4°C, rinsed 3 × 5 min with equal volumes of ND96, and then incubated for 1 h in a 1% BSA-ND96 blocking solution (used in subsequent antibody incubation steps). Fixed and blocked oocytes were incubated for 1 h in primary mouse anti-FLAG M2 (Sigma, Milan Italy) monoclonal antibody 1 µg/ml in 1% BSA-ND96, washed 6 × 3 min in 1% BSA-ND96, incubated for 1 h in secondary peroxidase-conjugated goat anti-mouse IgG 1 µg/ml, IgG-HRP (Jackson ImmunoResearch Laboratories), washed 6 × 3 min in 1% BSA-ND96 and then 6 × 3 min in ND96 alone. For chemiluminescence readings, each oocyte was transferred into a well of a 96-well plate (Assay Plate White not treated flat bottom, Corning Costar) filled with 50 µl SuperSignal Femto (Pierce); the washing solution was eliminated as much as possible. Chemiluminescence was quantified with a Tecan Infinity 200 microplate reader. The plates were read not later than 5 min after the transfer of the first oocyte. The data were then acquired at least

three times in 10 min, and for each oocyte the mean of three readings was calculated. Results were normalized to the mean value of wild-type FLAG-PepT1 for each batch and are given in relative light units (RLU).

Electrophysiology and data analysis

The two-electrode voltage-clamp technique (TEVC, GeneClamp, Axon Instruments Foster City, CA, or Oocyte Clamp OC-725B, Warner Instruments, Hamden, CT) was used throughout this work. Some experiments were conducted in current-clamp conditions, i.e., without strict voltage control, but with the possibility of constant current injections. Intracellular glass microelectrodes were filled with KCl 3 M and had tip resistances between 0.5 and 4 M Ω . Agar bridges (3% agar in 3 M KCl) connected the bath electrodes to the experimental chamber. In voltage-clamp mode the holding potential (V_h) was generally -60 mV, unless otherwise indicated. The standard protocol consisted of 200-ms-long pulses to test potentials from -140 to $+40$ mV in 20-mV increments. Other protocols including prepulses are described in the text. The current signal was filtered at 1 kHz before sampling at 2 kHz.

Data were analyzed using Clampfit 8.2 (Axon Instruments), and figures were prepared with Origin 5.0 (Microcal Software Inc., Northampton, MA).

Intracellular substrate injection

The non-hydrolyzable substrate Gly-Sar was used for confirmatory intracellular injection experiments. A volume of 50 nl of a concentrated solution (200 mM Gly-Sar in pH 7.5 buffer) was injected, leading to an approximate final concentration of 20 mM (assuming an oocyte volume of about 500 nl).

Solutions

The oocyte culture and washing solutions had the following compositions (in mM): ND96: NaCl 96, KCl 2, MgCl₂ 1, CaCl₂ 1.8, Hepes 5, pH 7.6; MBS: NaCl 88, KCl 1, NaHCO₃ 2.4, Hepes 15, Ca(NO₃)₂ 0.30, CaCl₂ 0.41, MgSO₄ 0.82, sodium penicillin 10 μ g/ml, streptomycin sulfate 10 μ g/ml, gentamycin sulfate 100 μ g/ml, nystatin 10 U/ml, pH 7.6; PBS: NaCl 138, KCl 2.7 Na₂HPO₄ 10, KH₂PO₄ 2, pH 7.6.

The external control solution had the following composition (mM): NaCl, 98; MgCl₂, 1; CaCl₂, 1.8. Different pH buffers were used for the various pH values: for pH 6.5, Mes 5 mM was used; Hepes 5 mM was employed for pH 7.0 and 7.5, whereas for pH 8.0 the buffer was Taps 5 mM. The final pH values were adjusted with HCl and NaOH.

Substrates were added at the indicated concentrations to the appropriate solutions. Irbesartan was from Sanofi-Aventis.

Experiments were performed at room temperature (20–25°C).

Results

Outward transport currents have been observed in wild-type PepT1 when depolarizing pulses of relatively short duration (50–250 ms) are applied with the voltage-clamp technique from negative (-40 , -60 mV) holding potentials [1, 2, 20]. Outward currents are most easily seen at alkaline pH and relatively low substrate concentrations, since increasing the concentration of either substrate or H⁺ shifts the current-voltage relationships to more positive potentials, eventually bringing the reversal potential (E_{rev}) out of the experimental range ([1] and our unpublished observations). In addition to the results in wild-type PepT1, we recently observed that some mutants in arginine 282 are capable of conducting quite large outward currents, as shown in Fig. 1.

The I/V relationships plotted in Fig. 1b show that in the same conditions of pH and substrate concentration the value of E_{rev} becomes progressively more negative as the positive charge of arginine is first neutralized to alanine and then changed in sign with aspartate. Moreover, the R282D mutant (but not R282A) generated significantly larger currents than the wild type. On the contrary, reverting the sign of the negative aspartate 341 to a positive arginine produces a transporter that is still functional but shows reduced transport currents and no reversal in the explored voltage range. In the group of oocytes illustrated in Fig. 1, the average currents at -140 mV were: 568 ± 58 nA for wild type, 998 ± 172 nA for R282D, 464 ± 94 nA for R282A, and 184 ± 35 for D341R (mean \pm SE, $n = 4-7$).

Another evident feature in the traces of the transport currents generated by the R282D and R282A mutants is the slow decline during the voltage pulse (arrows in Fig. 1a), a behavior that may suggest either the existence of a deactivating process or a progressive reduction in the driving force.

Figure 1c shows estimates of the surface expression of the various isoforms, obtained with the SOC method. The level of membrane localization is in good correlation with the transport-associated current in the case of the wild-type transporter and of the R282D and R282A mutants, but not for D341R, which, in spite of being highly expressed on the oocyte membrane, generates much smaller currents compared to the other isoforms. These observations suggest that the reduced functionality of D341R may be attributable to a

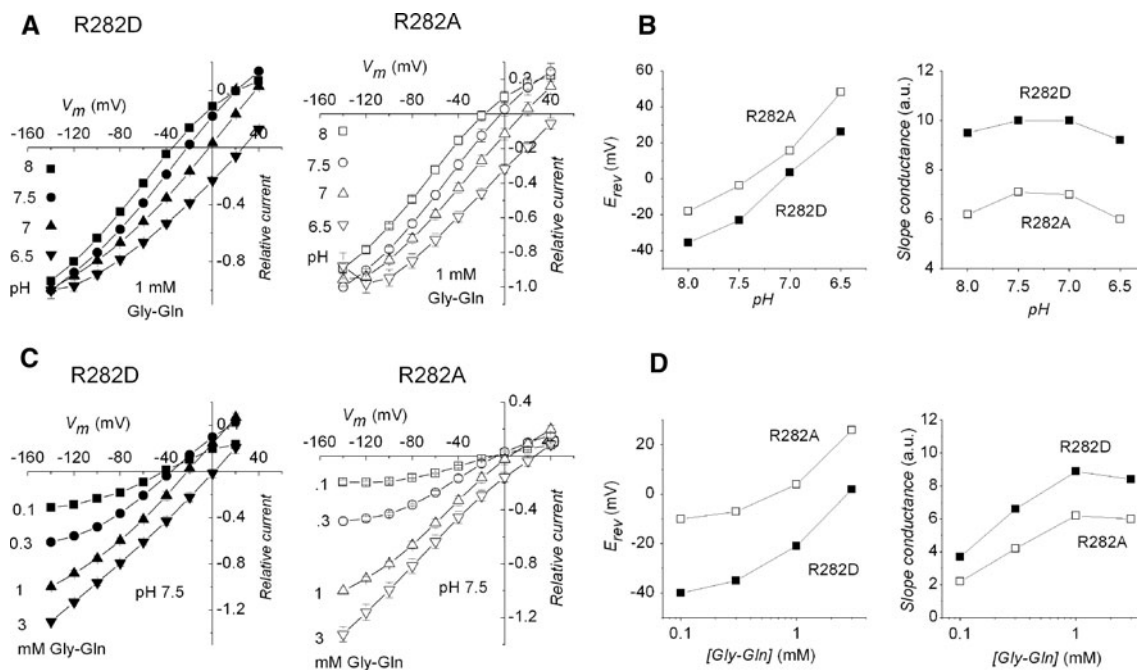


Fig. 2 *I/V* curves showing the effects of changing pH and substrate concentration on the R282D and R282A mutants. **A** External alkalization at fixed (1 mM) Gly-Gln concentration shifts the *I/V* curves towards more negative potentials. The change in E_{rev} with pH is shown in **B** for R282D (filled squares) and for R282A (open squares); these symbols are used throughout. No significant changes in the slope conductance at E_{rev} appear to be caused by alkalization. **C** Positive shifts in the *I/V* curves produced by increasing the external Gly-Gln concentration at fixed pH (7.5) in the two mutants. The shifts

in E_{rev} induced in this case are plotted in **D**, together with the slope conductance at E_{rev} ; this parameter shows an increase at higher Gly-Gln concentrations. The current data were averaged after normalization for each oocyte to the current value at -140 mV and pH 7.5. Data points are mean \pm SE ($n = 4\text{--}5$ from two batches). The slope conductance was calculated as the derivative of the relative *I/V* curve at E_{rev} . The value of E_{rev} for the R282A curve at pH 6.5 in **A** was linearly extrapolated

malfunctioning in the molecular mechanism rather than to defective targeting to the membrane.

In both R282D and R282A mutants the reversal potential of the transport current is shifted by changes in either the proton concentration or the substrate concentration (Fig. 2). This result suggests that the translocation of the two species occurs in a coupled fashion.

The shifts in E_{rev} caused by the pH and substrate changes in the mutants R282D and R282A are plotted in Fig. 2b and d. The slopes of the E_{rev} versus pH curve are -42.3 and -43.7 mV/pH unit, respectively; although less than the 58 mV/pH unit predicted for a pure H^+ current on the basis of the Nernst equation, these values are nevertheless consistent with a substantial contribution of H^+ to the current. Similarly, the semilog plots of E_{rev} versus [Gly-Gln] are not linear for both mutants (Fig. 2d) with even lower slopes compared to the pH dependence. We also estimated the slope conductance (g_{slope}) of the *I/V* curves at E_{rev} . This parameter is plotted in Fig. 2 as a function of pH and substrate concentration for both mutants. Interestingly, while g_{slope} increases with increasing concentrations of Gly-Gln (Fig. 2d), it appears to be substantially independent from the proton concentration (Fig. 2b). This last result is contrary to the

expectations for an electrodiffusive process, which would predict instead an increase in slope conductance when the concentration of the permeating species is raised [29].

Current reversal in the wild-type and R282 mutants

The apparently anomalous effects mentioned above on the slope conductance around E_{rev} prompted us to perform other experiments aimed at better understanding this phenomenon, both in the wild-type and in the R282D/A mutants. The necessity of further controls was also suggested by the declining behavior seen in the current traces in Fig. 1.

We performed long-lasting voltage- and current-clamp experiments on both wild-type and R282D mutants to investigate this point. Figure 3a shows voltage-clamp experiments in which the membrane voltage was stepped twice from -40 mV to $+40$ mV and back: the first step was given in the absence of substrate and the second in the presence of Gly-Gln 1 mM at pH 8. In these conditions, E_{rev} should be close to -30 mV in the R282D mutant. Figure 3Aa shows that jumping to $+40$ mV when the transporter is activated by 1 mM Gly-Gln causes an

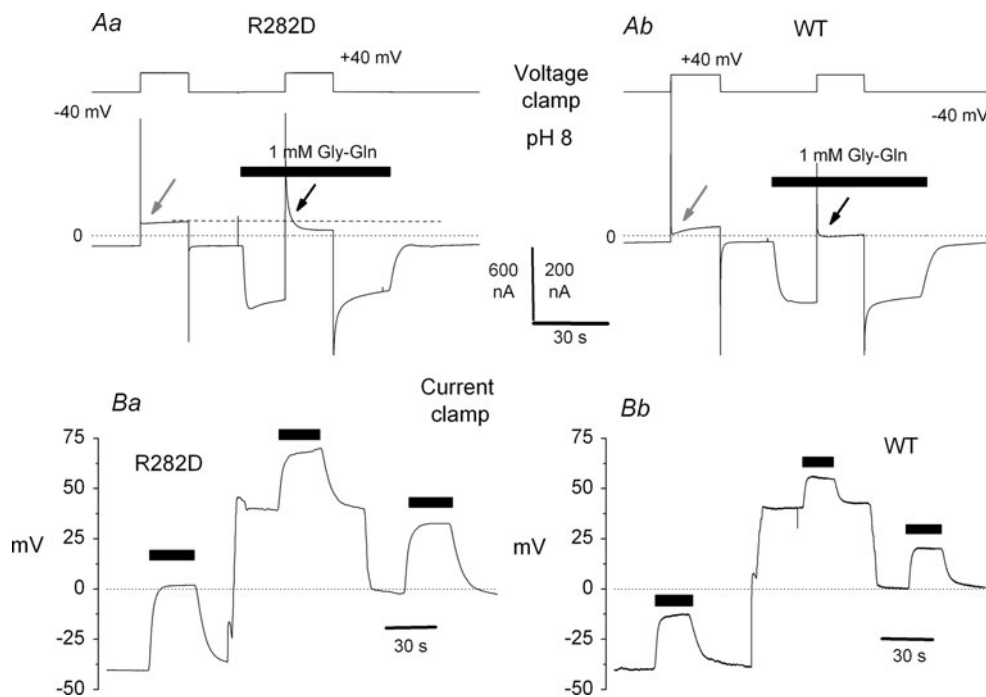


Fig. 3 *Aa* long-lasting records showing the slow deactivation process of R282D PepT1 following step voltage changes (*black arrow*): during the first seconds after the jump at +40 mV the current in the presence of substrate is more positive than in its absence (*gray arrow*); however, at later times it becomes more negative (the *dashed line* is drawn at the level of the current at +40 mV in the absence of substrate). *Ab* a less pronounced, but qualitatively similar behavior

was observed in the wild-type. *Ba* current clamp recordings at pH 8 in another oocyte expressing R282D PepT1; 1 mM Gly-Gln was added (*black bars*) while keeping the oocyte membrane at -40, +40, and 0 mV by current injection; in all three cases addition of substrate induced depolarizations, implying that an inward current was generated by the transporter. *Bb* same as in *Ba* from an oocyte expressing the wild-type transporter

instantaneous large outward current (*black arrow*) that declines with time constants in the order of fractions of seconds, and it is not seen in the absence of the substrate (*gray arrow*). Initially the current is more positive than the value recorded at the same voltage in absence of substrate (*dashed line*), but at the end of the 20-s period at +40 mV it becomes less positive (that is, a negative current after subtraction).

A qualitatively similar behavior, although with smaller currents, was observed in the wild-type PepT1 (Fig. 3Ab).

Figure 3b shows complementary experiments performed again on both wild type and R282D with analogous results. The oocytes were kept in current-clamp conditions, i.e., an appropriate current was injected to keep the membrane voltage at a desired value before substrate application, but the membrane potential was let free to change as a consequence of transporter operation. The representative traces in Fig. 3Ba, from an oocyte expressing R282D, and Fig. 3Bb, from an oocyte expressing wild-type PepT1, show that addition of 1 mM Gly-Gln at pH 8 (*black bars*) always induces a depolarization, irrespective of the starting value of the voltage (-40, 0, and +40 mV), indicating that the current generated by the transporter is in all cases in the inward direction.

The outward current is due to temporary accumulation of substrates

To discriminate whether the current decays seen in Figs. 1 and 3 were due to changes in electrochemical gradient or to a transporter-intrinsic deactivation process, a series of experiments employing different strategies was performed. Figure 4 illustrates the results of a representative experiment using a protocol in which three fast (200 ms) voltage ramps ranging from +40 to -100 mV (or from -140 to +40 mV) were superimposed on a long-lasting voltage step to +40 (or -140) mV in conditions inducing the decay of the transport current in both directions (pH 8, 1 mM Gly-Gln).

As shown in Fig. 4Ac and Bc, the *I/V* curves derived from the ramps shift along the voltage axis according to the application order and to the level of the long-lasting voltage pulse. The ramps superimposed on the depolarizing (+40 mV) pulse exhibit a progressive shift toward more positive potentials (Fig. 4Ac), whereas those applied during the pulse to -140 mV are moved with time toward more negative potentials (Fig. 4Bc). Interestingly, in both cases the curves remain parallel to each other, so that it may be concluded that only the reversal potential is affected, not the conductance.

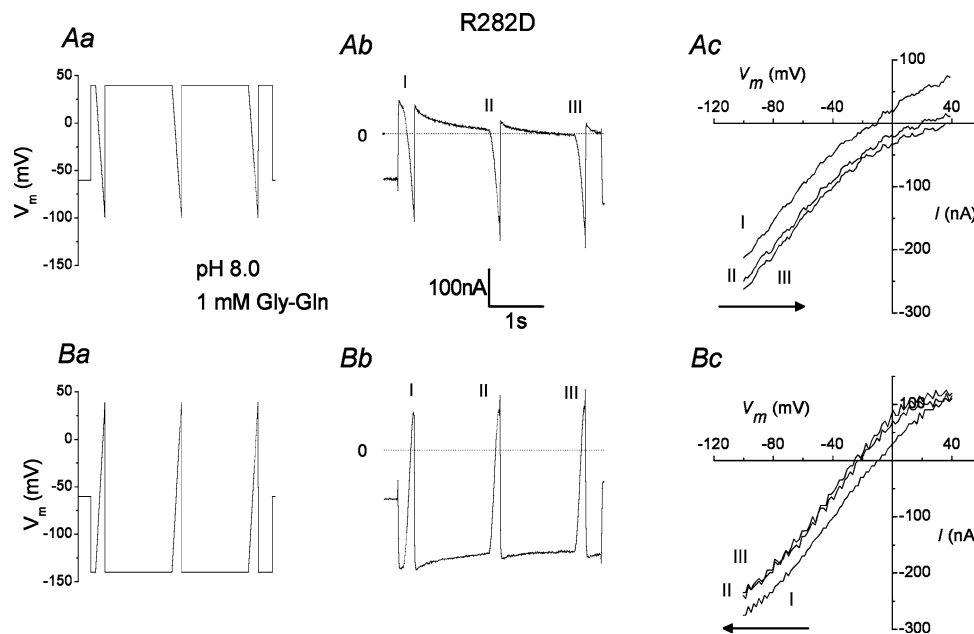


Fig. 4 Step and ramp protocols to investigate the basis of the transport current decline. Three fast (200 ms) ramps are superimposed on long-lasting pulses to +40 mV (*Aa*) or -140 mV (*Ba*). *Ab* and *Bb* show the subtracted (substrate minus control) transport currents elicited by the two protocols in a representative oocyte expressing R282D at pH 8.0 upon addition of 1 mM Gly-Gln. Both

records show the slowly declining currents, which are in the outward direction in *Ab* and in the inward direction in *Bb*. In *Ac* and *Bc* the *I/V* relationships obtained from the ramps are plotted. In *Ac* the reversal potential moves toward more positive values with the second and third ramp, whereas in *Bc* the opposite behavior is observed. In both graphs the *I/V* curves remain substantially parallel to each other

These observations represent a strong indication that the decline of the transport current during either the depolarizing or the hyperpolarizing pulses is due to substrate concentration changes in the vicinity of the transporters.

In fact, assuming that E_{rev} might be written as a Nernst equation for the proton-substrate complex:

$$E_{rev} = \frac{RT}{F} \ln \frac{[TC]_{out}}{[TC]_{in}}$$

where TC stands for *transported complex*, the continuous inward flow during the hyperpolarizing pulse will increase $[TC]_{in}$ (and/or decrease $[TC]_{out}$), causing E_{rev} to change with time to more negative values, as observed in Fig. 4Bc. On the contrary, the initial outward current seen when stepping the potential from -60 to +40 mV (Fig. 4Ab) will decrease $[TC]_{in}$ (and/or increase $[TC]_{out}$), shifting E_{rev} to more positive potentials (Fig. 4Ac).

On the whole, the results shown in Fig. 4 indicate that the outward current seen during short depolarizations is caused by a local accumulation of the transported complex at the intracellular side of the membrane and/or a local depletion of the complex at the extracellular side during the continuous inward transport occurring at the negative holding potential, confirming earlier suggestions [20].

In another series of experiments a prepulse lasting 2 s to +40 mV from $V_h = -40$ mV was applied to the membrane before moving the potential to variable 1-s-long test

pulses (+40 to -140 mV). Figure 5 shows this kind of protocol applied to an oocyte expressing the R282D mutant at pH 7.5. Upon addition of 3 mM Gly-Gln, a slowly declining outward current is seen during the prepulse, whereas an opposite behavior (i.e., a slowly declining inward current) is observed at the most negative test pulse potentials (Fig. 5a middle traces). Subtraction of the currents in the absence from those in the presence of substrate gives the isolated transport currents (Fig. 5a rightmost traces), in which the declining behavior at negative potentials during the test pulses is still visible. The average *I/V* relationship obtained from the currents values at the end of the test pulses is plotted in Fig. 5c (open squares). It can be seen that using this protocol no outward current can be observed up to +40 mV. In contrast, a clear current reversal around +10 mV is noticeable in the same conditions of pH and Gly-Gln concentration when using the short depolarizing pulses from $V_h = -60$ mV (filled squares in Fig. 5c).

This experiment indicates that during the prepulse to +40 mV the accumulation/depletion effects are dissipated.

To check the physiological relevance of this phenomenon, a similar approach was applied to oocytes expressing the wild-type form of PepT1. In this case a shorter (250 ms) prepulse to +40 mV was sufficient to abolish the temporary phase of the outward current (Fig. 6).

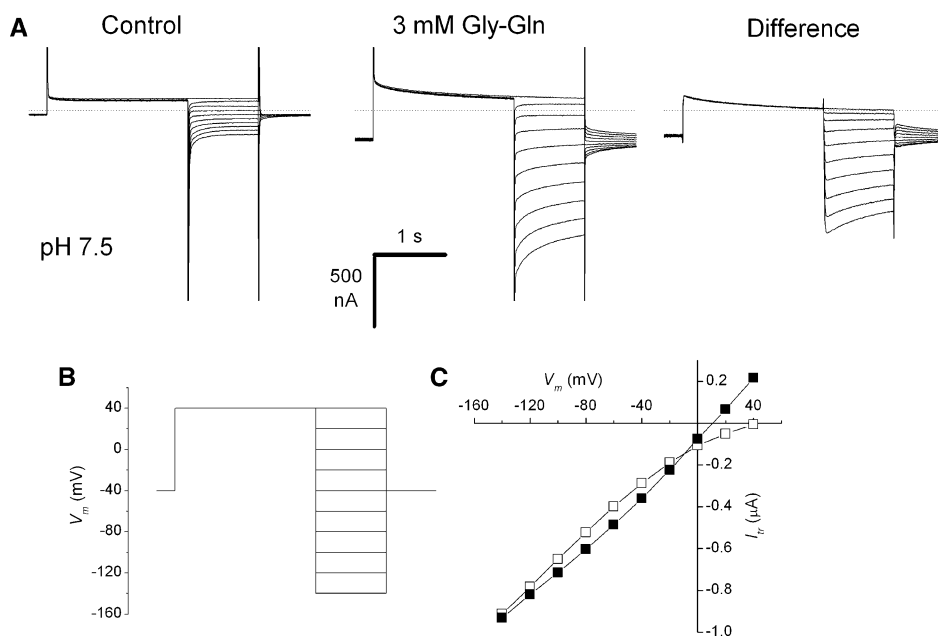


Fig. 5 **A** Currents elicited by the prepulse protocol shown in **B**, in the absence and in the presence of 3 mM GlyGln at pH 7.5 in an oocyte expressing the R282D isoform; the last traces are the difference (substrate minus control). The *dotted lines* represent the zero-current

level. **C** Plot of the current at the end of the test pulse in Ac (*open symbols*); for comparison, the *filled symbols* are the data obtained using the short-duration pulse protocol (from V_h -60 mV) from another oocyte in the same conditions

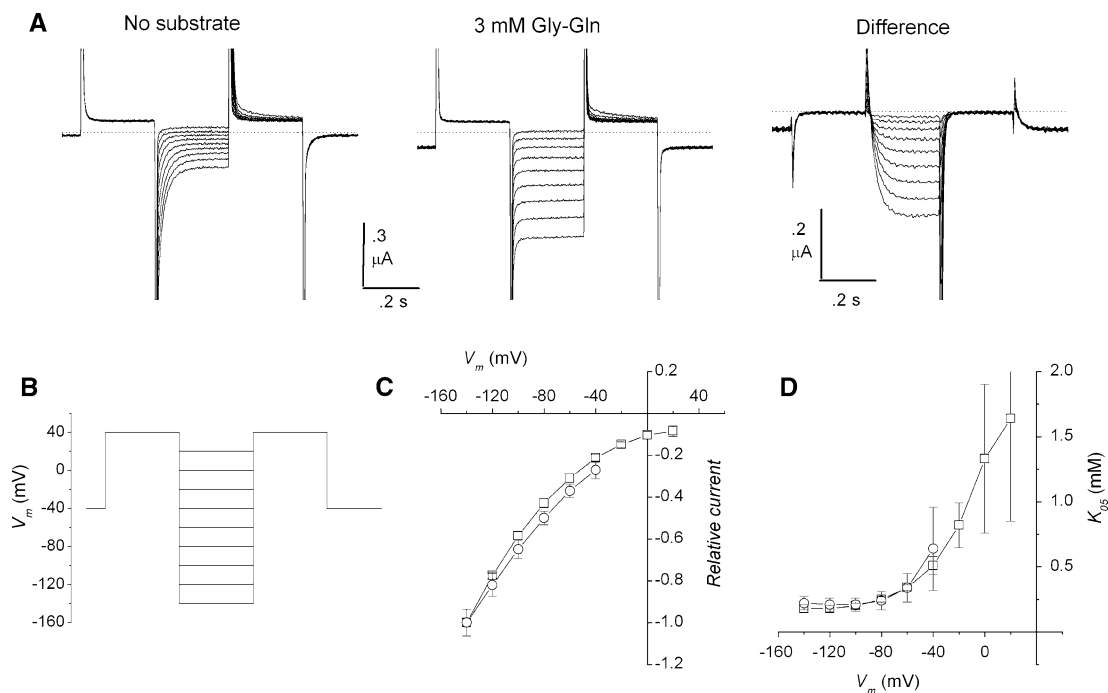


Fig. 6 Transport currents with the prepulse protocol. In this protocol a 250-ms prepulse to $+40$ mV precedes the pulses to the test potentials (**B**, data from the postpulse to $+40$ mV were not used for analysis). In the wild-type PepT1 this prepulse duration was sufficient to abolish any outward current elicited by the jump from the -60 mV holding potential to positive potentials. This is demonstrated by the fact that the subtracted currents (**A**, rightmost traces) are all in the inward direction (the *dotted line* indicates the zero current level).

C, **D** Values of maximal current (I_{max}) and substrate concentration giving half I_{max} ($K_{0.5}$) obtained by Michaelis—Menten analysis on dose-current curves obtained using the prepulse protocol (open squares, mean \pm SE, $n = 4$ from two batches). For comparison, the same parameters calculated with the usual protocol (no prepulse) are shown (open circles, mean \pm SE, $n = 6$ from two batches); notice the limitation at -40 mV. I_{max} was normalized to the value at -140 mV in each oocyte before averaging

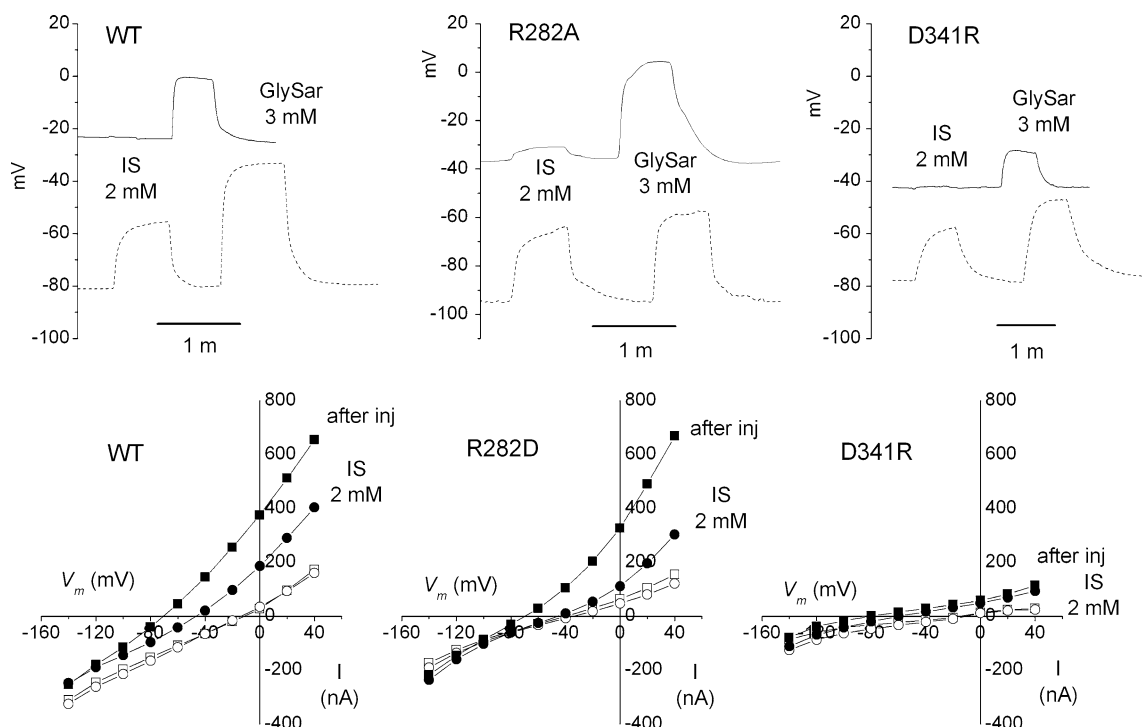


Fig. 7 Top row current-clamp recordings showing the resting potential changes induced by application of Irbesartan (IS, 2 mM) and Gly-Sar (3 mM) to representative oocytes expressing the indicated isoforms before (solid trace) and after the intracellular injection of Gly-Sar (dashed trace). The bottom graphs show the

corresponding uncorrected I/V relationships, before (open symbols) and after (filled symbols) the injection of Gly-Sar. In all graphs squares are data in the absence and circles in the presence of Irbesartan

The transport-associated currents, obtained as usual by subtracting the traces in the absence from those in the presence of substrate, were always inwardly directed, even in conditions of alkaline pH and low organic substrate concentrations (Fig. 6a, rightmost traces). This correction, although modest, allows an extension of the voltage range in which the values of apparent affinity ($1/K_{05}$) and maximal current (I_{max}) can be obtained from a Michaelis–Menten analysis.

The average values of K_{05} and I_{max} calculated from a group of oocytes tested with such protocol at pH 7.5 are shown in Fig. 6c and d (open squares), together with their counterpart obtained using the customary pulse protocol in which the test pulses were applied directly from $V_h = -60$ mV without prepulse (open circles). It can be seen that while the data from the classical protocol are limited to -40 mV, because at more positive potentials the current at low substrate concentration becomes outwardly directed, the prepulse protocol allows an extension of the analysis up to $+20$ mV, although for K_{05} the statistical error becomes very large also in this case.

Intracellular injection of substrates

In order to find further support for the results reported above, we performed a series of experiments injecting

substrates in the cytoplasm of the oocyte. This procedure has already been reported to produce significant outward transport currents in wild-type PepT1 when using hydrolysis-resistant dipeptides or inhibiting intracellular peptidases [2]. The results of our experiments on the wild-type and R282D, R282A and D341R isoforms are illustrated in Fig. 7. In the upper part of this figure membrane voltage recordings in current-clamp condition are shown: first of all it can be noted that in all isoforms the resting membrane potential becomes significantly more negative after substrate injection (range -75 to -100 mV) compared to the initial -20 to -50 mV. This progressive hyperpolarization, already observed in the wild type [2], develops in a few minutes after injection, and it is not observed in oocytes not expressing the transporters. The development of a strongly negative resting potential is clearly consistent with the activation of an outward current by the transporter as a consequence of the increased intracellular Gly-Sar concentration. Additional evidence is provided by the application of the blocker Irbesartan (IS) [30]: the traces in Fig. 7 show that while external Gly-Sar 3 mM depolarizes the membrane when applied either before or after the intracellular injection, the application of Irbesartan (2 mM) is effective in producing a depolarization only after substrate injection. These last observations indicate that, while the depolarizations induced by external

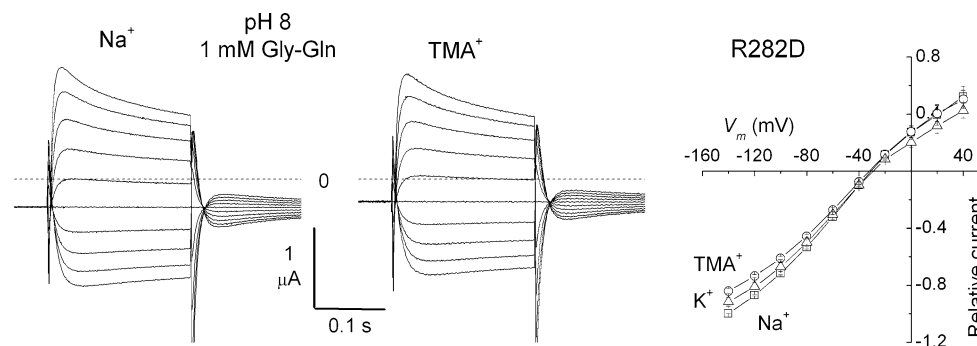


Fig. 8 Replacement of Na⁺ with TMA⁺ or K⁺ in the external solution did not significantly alter the amplitude or the reversal potential of the transport current elicited by the organic substrate.

Values in the *I/V* plot are mean \pm SE from six oocytes from two batches. Currents were normalized to the value at -140 mV in Na⁺ for each oocyte before averaging

Gly-Sar are due to the development of an inward transport current, those induced by Irbesartan are due to the inhibition of an outward current.

Interestingly, the hyperpolarization of the resting membrane potential and the Irbesartan-induced depolarization are seen in all isoforms, including D341R, in spite of the much lower currents generated by this mutant.

The *I/V* curves in Fig. 7 confirm then the findings reported in the preceding figures by showing the presence of a strong outward current following the intracellular injection of Gly-Sar and a reduction of this current by Irbesartan.

Ion and substrate specificity

Previous results [17–19] have suggested that residues R282 and D341 form an ion bridge whose cyclic breaking and formation may gate the translocation process. Furthermore, it has been proposed [31] that PepT1 may represent a transitional entity between transporters and channels. We have thus investigated possible alterations in ion and substrate specificity in the R282D mutant (the same results were obtained in R282A as well). The possible participation of other cations in the current elicited by the organic substrate was tested by replacing external Na⁺ with K⁺, Li⁺, or tetramethylammonium ion (TMA⁺). However, these ionic substitutions did not significantly alter the shape of the *I/V* relationships in the presence of Gly-Gln at various concentrations and pH values, as shown in Fig. 8 for pH 8 and Gly-Gln 1 mM. It can be seen that the reversal potential and the outwardly directed current are independent of the kind of cation representing the vast majority of external positive charges.

This result together with the observations in Fig. 2 confirms therefore that the species carrying the electrical charge in both directions are indeed protons in complex with the organic substrate.

The substrate selectivity of R282D was also compared with that of the wild type with special attention to the ability to generate reverse current. A first series of results is exemplified in Fig. 9, where the capacity to transport di-, tri-, and tetrapeptides, as well as histidine by the R282D mutant was tested. It is known [22, 23] that PepT1 family members are able to transport several di- and tripeptides, but not tetrapeptides. Furthermore, among the SLC15A family of transporters, the PepT subfamily is differentiated from the PHT subfamily by its inability to transport histidine. The representative records of Fig. 9a show that, with respect to substrate selectivity, R282D behaves in a manner similar to the wild-type transporters. The same potency order was found in the other two tested mutants, R282A and D341R (not shown). Furthermore, as illustrated in Fig. 9b, tripeptides (LGG) are also able to generate outward current when the short pulse protocol from $V_h = -60$ mV is used.

Charged dipeptides

In the context of the substrate selectivity analysis, it seemed particularly interesting to examine the behavior of the mutants in the charge-pair residues when charged dipeptides were used in place of the neutral substrates employed in all previous experiments.

The relevance of introducing a negative or a positive amino acid in the substrate dipeptide as well as its position was already studied in the wild-type PepT1 [32, 33]. An important conclusion from these studies was that the binding pocket of PepT1 can accept only neutral amino acids at the carboxy terminus, while at the amino terminus all kinds of charges can be accommodated.

Figure 10 compares the transport currents generated at the same pH (7.5) and substrate concentration (1 mM) when a positive or a negative residue is introduced in either position of the dipeptide. The transport currents were

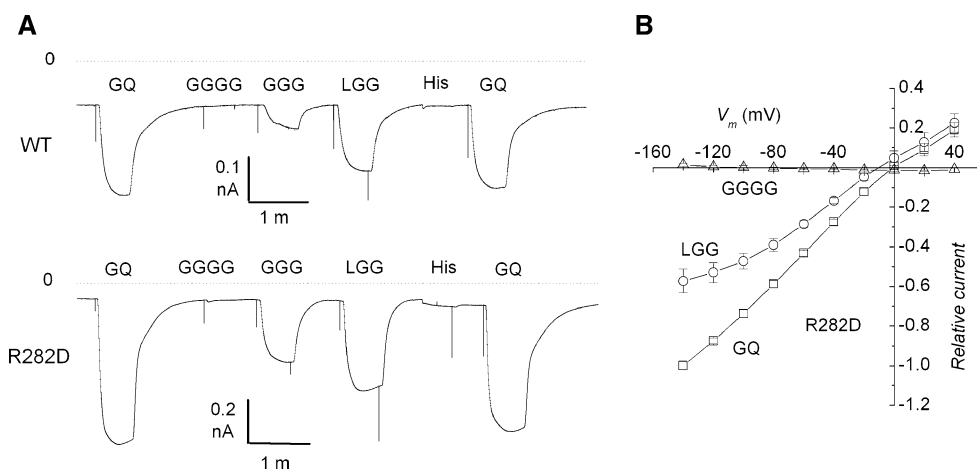


Fig. 9 **A** Representative records comparing the relative efficiency to elicit transport current by di-, tri-, and tetrapeptides and histidine in the wild-type and in the R282D mutant (*GQ* gly-gln, *GGGG* tetraglycine, *GGG* triglycine, *LGG* leu-gly-gly, *His* histidine); the dotted lines indicate the zero-current level. **B** Average *I/V* relationship

showing the outward current generated by the dipeptide *GQ*, the tripeptide *LGG*, and the lack of tetrapeptide-induced current in the R282D mutant. Data (mean \pm SE) were normalized to the *GQ* value at -140 mV for each oocyte before averaging. Substrate concentration 1 mM, pH 7.5

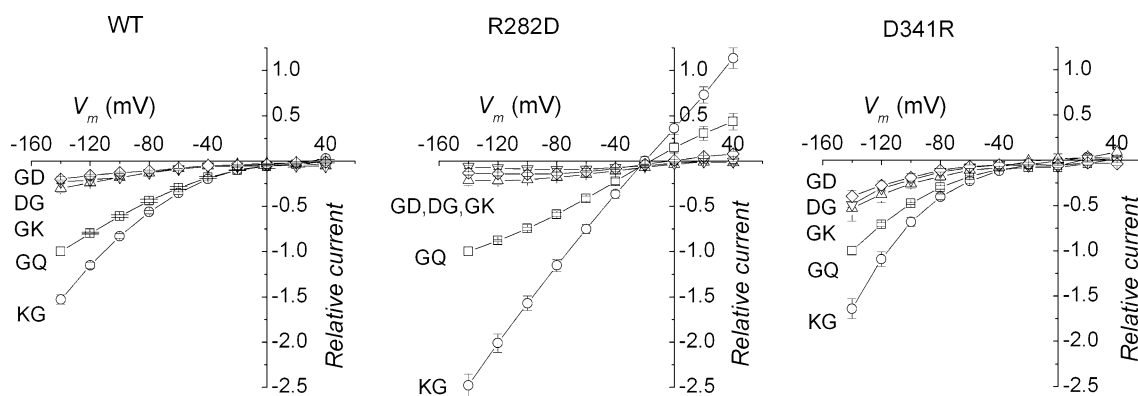


Fig. 10 Current-voltage relationships of the transport currents elicited by differently charged dipeptides in comparison with Gly-Gln (all at 1 mM) in the indicated isoforms at pH 7.5. Data are averages (after

normalization at the current elicited by *GQ* at -140 for each oocyte) \pm SE from 5 to 8 oocytes for each group, three batches)

normalized to the current generated by the neutral dipeptide Gly-Gln at -140 mV in each oocyte before averaging. The previous observations on the wild type are qualitatively confirmed in the mutants: the transport currents generated by Lys-Gly are larger compared to Gly-Gln in all isoforms, while those produced by Gly-Lys and by the two negatively charged dipeptides are smaller. However, the degree of reduction or increase is different in the two mutants: in the R282D the differences are enhanced Lys-Gly showing a much larger increase (150% vs 60% in the wild type), whereas the currents generated by Gly-Lys, Gly-Asp, and Asp-Gly are reduced relatively more than in the wild type. In the D341R form, which produces in general smaller currents (see Fig. 1), the Gly-Lys, Gly-Asp, and Asp-Gly currents are less strongly reduced, and the Lys-Gly current increases similarly to the wild type.

Furthermore, Lys-Gly can produce large outward currents in R282D, whereas all substrates produce strongly inward-rectifying currents in D341R.

The results for the wild-type are in line with previous observations [32, 33], and qualitatively reflect the excess positive or negative charge of the different dipeptides at pH 7.5. The more than doubled slope of the *I/V* curves in the R282D mutant can be best explained with a nearly doubled charge/mole ratio and, in addition, with an increased turnover rate of the transporter.

On the contrary, the lack of effect in the substrate selectivity order suggests that these mutations do not interfere with the binding pocket of the transporter.

We tested this prediction by evaluating the amount of presteady-state charge movement removed by interaction with the various dipeptides. It is known that in many

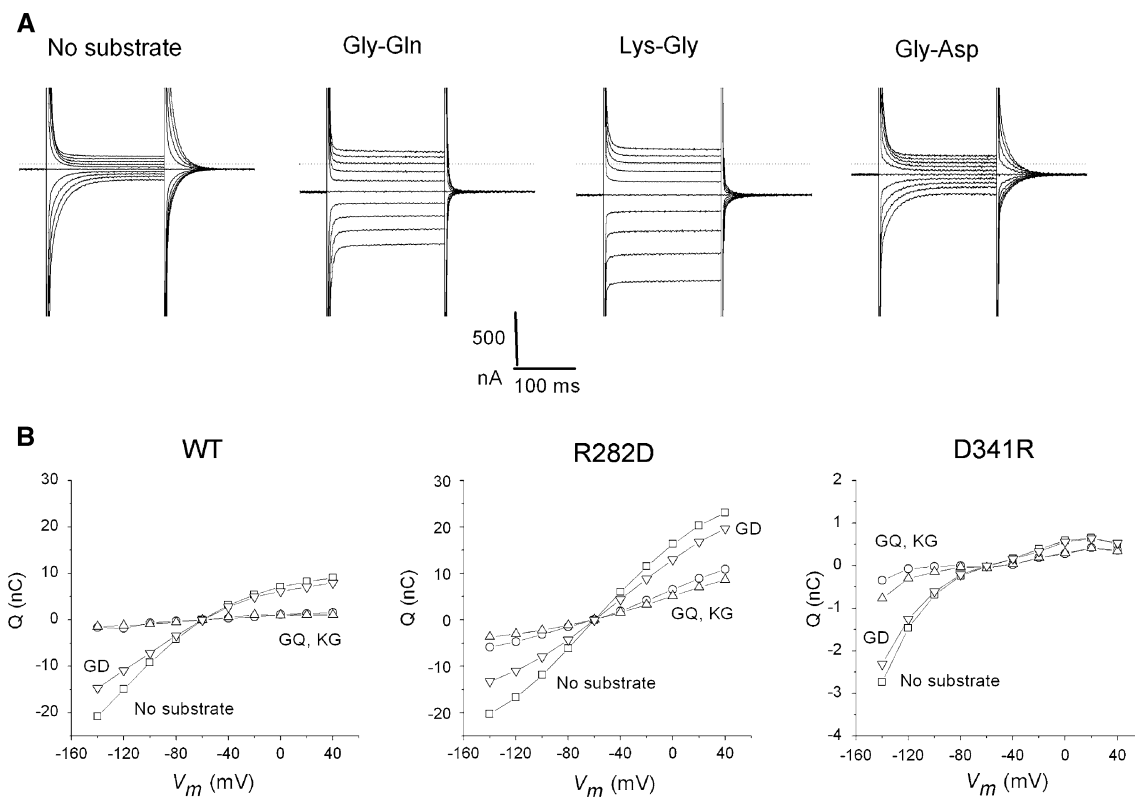


Fig. 11 Residual charge movement. The *upper row* shows current records from an oocyte expressing wild-type PepT1 in the absence and presence of a neutral, a basic, and an acidic dipeptide as indicated (all at concentration 1 mM and pH 7.5). The appearance of the steady transport current is inversely related to the disappearance of the

presteady-state currents. The *bottom graphs* show, for the wild-type and the R282D and D341R mutants, the voltage dependence of the total charge movement (*squares*) and the residual charge movement in the presence of the substrate (*circles* GQ, *upward triangles* KG, *downward triangles* GD)

transporters, including PepT1 [34, 35], the presteady-state currents in the absence of substrate are mutually exclusive with the transport currents (i.e., they are progressively reduced with corresponding increases in transport current). Figure 11 shows the residual charge movement in the presence of 1 mM of different dipeptides (Gly-Gln, Lys-Gly, and Gly-Asp) in representative oocytes expressing the wild type and the mutants R282D and D341R.

As shown in the traces of Fig. 11, 1 mM Gly-Gln and Lys-Gly almost completely remove the presteady-state currents in the wild type, whereas most of this kind of current remains in the presence of the same amount of Gly-Asp (the same result was observed with Asp-Gly and Gly-Lys). These observations may be quantified by comparing the Q/V curves obtained by integrating the presteady-state current isolated using a double exponential fitting of the traces in the absence of substrate (considered to represent the total charge) to the integrals of the transient currents obtained by the difference of the traces in the absence and in presence of substrate (residual charge) [36]. These data are shown in the bottom graphs of Fig. 11. Clearly the residual charge in the presence of 1 mM

Gly-Gln and Lys-Gly is close to zero in the wild type, and for these substrates it remains a small fraction of the total charge in both mutants. In contrast, for Gly-Asp the residual charge is close to the total charge in all isoforms. Analogous results were obtained for the other, poorly functional dipeptides (not shown).

The amount of residual charge can be considered an estimate of the fraction of transporters not involved in the actual transport, i.e., transporters that do not interact with the substrate. In this view, the data of Fig. 11 indicate that for all isoforms Gly-Asp interacts poorly, whereas Gly-Gln and Lys-Gly show a comparable degree of interaction between each other, although in the mutants this level appears lower than in the wild type.

Taking together the results of Figs. 10 and 11, it can be concluded that, since the level of interaction of Gly-Gln and Lys-Gly with the R282D mutant is similar, the more than twofold increase in transport current by Lys-Gly should be ascribed to the increased charge/mole ratio of the transported complex and possibly to an increased turnover rate.

Discussion

The PepT1 mutants investigated in the present work are correctly expressed in the oocyte membrane (Fig. 1) and maintain the characteristic of true cotransporters, as is shown by the fact that both protons and substrate concentrations affect the reversal potential of the transport current (Fig. 2) and that the substrate selectivity is unaltered. Although qualitatively in the correct direction, the shifts in E_{rev} significantly deviate from the predictions of the Nernst equation. Further difficulties arise when examining the slope conductance of the transport current at the reversal potential: according to the theory of electrodiffusion [29] this parameter should increase when the concentration of the diffusing species is increased. As shown in Fig. 2 this is verified for the dipeptide substrate Gly-Gln, but not for protons, for which no significant dependency of the g_{slope} is found.

Having established that R282D and R282A can be considered as true cotransporters with some interestingly altered properties (conspicuous outward currents), we investigated the functional and structural determinants of reverse operation in these proteins.

The experiments illustrated in Fig. 3 show that the outward currents visible in Figs. 1 and 2 are only temporary and may be consequent to the active state of the transporters at negative holding potentials. These declining outward currents might be considered similar to the “tail” currents observed in voltage-activated ionic channels when stepping the voltage from a condition in which the channel is open to other voltages where it will close [29, 37]. If this is the case, the I/V curves obtained from relatively short (<1 s) pulses may actually represent “instantaneous” I/V relationships of the current generated by the transporter at the level of activation of the holding potential.

The observation (Figs. 1 and 4) that the transport current declines during strong voltage pulses in either depolarizing or hyperpolarizing directions suggests that this effect may arise from changes in the driving force rather than from an intrinsic deactivation process of the transporter, because this last kind of process usually depends monotonically on voltage. The hypothesis of a reduction in driving force is demonstrated by the results of the experiments of Figs. 4, 5, and 6, as well as from the long-lasting recordings of Fig. 3. In fact, during a prolonged flux of the proton-substrate complex a local accumulation and/or depletion of the complex may occur in the vicinity of the transporter, and this will decrease the concentration-dependent component of the electrochemical gradient causing a current decline.

The experiment of Fig. 4 clearly demonstrates the occurrence of this phenomenon in both directions: in fact, during a long-lasting hyperpolarization the reversal potential becomes progressively more negative in

agreement with a decrease in the out/in ratio of the concentrations of the transported species (Eq. 1). Vice versa, during a long-lasting depolarization, the E_{rev} shift is toward more positive potentials, consistent with an increase in the out/in concentration ratio. However, the I/V relationships measured at different times during the long pulses in either direction remain parallel to each other, excluding changes in the intrinsic rate of transport.

Although this effect is most evident in the two arginine 282 mutants, we have shown that the hypothesis of a transport-dependent local concentration change can also explain the findings regarding the wild-type transporter [20]. The experiments of Figs. 5 and 6 show that using an appropriate protocol the accumulation/depletion effect can be reduced, and this leads to more accurate determinations of the kinetic properties of transport (I_{max} and $K_{0.5}$), whose values can be obtained over an extended range of membrane potentials.

The ability to conduct current in the outward direction was already demonstrated in the wild-type PepT1 [2]. We have shown here that not only mutants in arginine 282, but also D341R exhibit the same capacity in presence of high intracellular concentrations of a non-hydrolyzable substrate. This finding indicates that the different shape of the I/V curves exhibited by the different isoforms (i.e., inward rectifying vs linear, see Figs. 1 and 10) obtained using a classical pulse protocol from $V_h = -60$ mV is not related to an intrinsic incapacity of the wild-type and D341R forms to transport in reverse mode, but depends on the different transport rates, producing different degrees of accumulation/depletion effects. Indeed the transformation from linear to inward rectifying can be obtained using appropriate protocols (see Fig. 5).

Other substrates

Of the two residues forming a putative charge pair in the PepT1 structure (R282 and D341), [17, 18], only mutants in arginine 282 present the outward current phenotype (Fig. 1). Our initial results using the neutral dipeptide Gly-Gln showed that the arginine mutants facilitate the substrate flow both in terms of amplitude and direction, since the I/V relationships are approximately linear, whereas the symmetric mutation D341R has an opposite action, rendering more difficult the transport of substrates and enhancing the inward rectification property already present in the wild type.

The subsequent experiments in the presence of different cations (Li^+ , K^+ and TMA^+) and using various organic substrates showed that the mutations do not introduce qualitative alteration in ionic selectivity nor in substrate specificity. Protons appear to remain the charge carriers, and the potency order of substrates of different size or

bearing different charge is not changed compared to the wild type.

Furthermore, the reversal of the transport current can also be observed with tripeptides, suggesting that this property is not substrate-dependent, but is intrinsic in the mutated transporter.

The selectivity order of the charged dipeptides remains substantially unaltered in the mutants compared to the wild-type at pH 7.5. The two negatively charged dipeptides produce only small currents, reflecting the high percentage of the side chains bearing a negative charge at this pH. The two positive dipeptides highlight the relevance of the position of the charge: when the lysine is at the amino terminus, the transporter is able to generate larger currents, while when it is located at the carboxy terminus, the currents are much reduced [33].

Quantitatively, the behavior of the charge-reverting mutants R282D and D341R is opposite in many respects: while R282D shows increased current relative to the wild type, the current generated by D341R is much reduced (see Fig. 1 and related text). This observation is consistent with the idea of these two residues being part of the gate controlling the flux of inward positive charges: neutralization of the positive arginine 282, or its replacement with a negative amino acid, may facilitate the approach of the positively charged transport complex, whereas the replacement of the negative aspartate 341 with a positive arginine may have the opposite effect. This notion is also supported by the amplified increase (relative to Gly-Gln) in the current generated by Lys-Gly in the R282D mutant compared to wild type and D341R. This effect is mirrored by the stronger reduction in the same mutant of the current generated by Asp-Gly compared to the wild type. Interestingly, this last substrate produces a higher fraction of the Gly-Gln current in the D341R mutant compared to the wild type.

In conclusion, we have shown that mutants in the putative charge pair residues R282 and D341 of rabbit PepT1, while retaining the essential characteristics of proton-coupled cotransporters, exhibit properties useful to better understand the possibility of reverse transport. Removal of arginine 282 appears to facilitate the flow of the transported complex in both directions, while replacement of aspartate 341 with a positive residue limits the transport rate and strengthens the inwardly rectifying characteristics of the wild-type transporter.

Acknowledgments Many thanks are due to Dr. Stefano Giovannardi for skillful technical assistance. This work was supported by the University of Insubria Research Fund.

References

- Verri T, Kottra G, Romano A, Tiso N, Peric M, Maffia M, Boll M, Argenton F, Daniel H, Storelli C (2003) Molecular and functional characterization of the zebrafish (*Danio rerio*) PEPT1-type peptide transporter. *FEBS Lett* 549:115–122
- Kottra G, Frey I, Daniel H (2009) Inhibition of intracellular dipeptide hydrolysis uncovers large outward transport currents of the peptide transporter PEPT1 in *Xenopus* oocytes. *Pflug Arch* 457:809–820
- Rühl A, Hoppel S, Frey I, Daniel H, Schemann M (2005) Functional expression of the peptide transporter PEPT2 in the mammalian enteric nervous system. *J Comp Neurol* 490:1–11
- Rossi DJ, Oshima T, Attwell D (2000) Glutamate release in severe brain ischaemia is mainly by reversed uptake. *Nature* 403:316–321
- Khoshbouei H, Wang H, Lechleiter JD, Javitch JA, Galli A (2003) Amphetamine-induced Dopamine efflux. A voltage-sensitive and intracellular Na-dependent mechanism. *J Biol Chem* 278:12070–12077
- Seidel S, Singer EA, Just H, Farhan H, Scholze P, Kudlacek O, Holy M, Koppatz K, Krivanek P, Freissmuth M, Sitte HH (2005) Amphetamines take two to tango: an oligomer-based counter-transport model of neurotransmitter transport explores the amphetamine action. *Mol Pharmacol* 67:140–151
- Richerson GB, Wu Y (2003) Dynamic equilibrium of neurotransmitter transporters: not just for reuptake anymore. *J Neurophys* 90:1363–1374
- Richerson GB, Wu Y (2004) Role of the GABA transporter in epilepsy. *Adv Exp Biol* 548:76–91
- Meredith D, Price RA (2006) Molecular modeling of PepT1—towards a structure. *J Membr Biol* 213:79–88
- Krishnamurthy H, Piscitelli CL, Gouaux E (2009) Unlocking the molecular secrets of sodium-coupled transporters. *Nature* 459:347–355
- Abramson J, Wright EM (2009) Structure and function of Na(+)-symporters with inverted repeats. *Curr Opin Struct Biol* 19:425–432
- Terada T, Saito H, Mukai M, Inui K (1996) Identification of the histidine residues involved in substrate recognition by a rat H⁺/peptide cotransporter, PEPT1. *FEBS Lett* 394:196–200
- Fei Y-J, Liu W, Prasad PD, Kekuda R, Oblak TG, Ganapathy V, Leibach FH (1997) Identification of the histidyl residue obligatory for the catalytic activity of the human H⁺/peptide cotransporters PEPT1 and PEPT2. *Biochemistry* 36:452–460
- Chen X-Z, Steel A, Hediger MA (2000) Functional roles of histidine and tyrosine residues in the H⁺-peptide transporter PepT1. *Biochem Biophys Res Comm* 272:726–730
- Yeung AK, Basu SK, Wu SK, Chu C, Okamoto CT, Hamm-Alvarez SF, Von Grafenstein H, Shen WC, Kim JK, Bolger MB, Haworth IS, Ann DK, Lee VHL (1998) Molecular identification of a role for tyrosine 167 in the function of the human intestinal proton-coupled dipeptide transporter (hPepT1). *Biochem Biophys Res Comm* 250:103–107
- Kulkarni AA, Haworth IS, Uchiyama T, Lee VHL (2003) Analysis of transmembrane segment 7 of the dipeptide transporter hPepT1 by cysteine-scanning mutagenesis. *J Biol Chem* 278:51833–51840
- Kulkarni AA, Davies DL, Links JS, Patel LN, Lee VHL, Haworth IS (2007) A charge pair interaction between Arg282 in transmembrane segment 7 and Asp341 in transmembrane segment 8 of hPepT1. *Pharmaceut Res* 24:66–72

18. Pieri M, Hall D, Price R, Bailey P, Meredith D (2008) Site-directed mutagenesis of arginine 282 suggests how protons and peptides are co-transported by rabbit PepT1. *Int J Biochem Cell Biol* 40:721–730
19. Meredith D (2004) Site-directed mutation of arginine 282 to glutamate uncouples the movement of peptides and protons by the rabbit proton-peptide cotransporter PepT1. *J Biol Chem* 279:15795–15798
20. Kottra G, Daniel H (2001) Bidirectional electrogenic transport of peptides by the proton-coupled carrier PEPT1 in *Xenopus laevis* oocytes: its asymmetry and symmetry. *J Physiol* 536:495–503
21. Vig BS, Stouch TR, Timoszyk JK, Quan Y, Wall DA, Smith RL, Faria TN (2006) Human PEPT1 pharmacophore distinguishes between dipeptide transport and binding. *J Med Chem* 49:3636–3644
22. Herrera-Ruiz D, Knipp GT (2003) Current perspectives on established and putative mammalian oligopeptide transporters. *J Pharmacol Sci* 92:691–714
23. Daniel H, Spanier B, Kottra G, Weitz D (2006) From bacteria to man: archaic proton-dependent peptide transporters at work. *Physiology* 21:93–102
24. Mertl M, Daniel H, Kottra G (2008) Substrate-induced changes in the density of peptide transporter PEPT1 expressed in *Xenopus* oocytes. *Am J Physiol Cell Physiol* 295:1332–1343
25. Bossi E, Fabbrini MS, Ceriotti A (2007) Exogenous protein expression in *Xenopus laevis* oocyte, basic procedure. *Methods Mol Biol* 375:107–131
26. Zerangue N, Schwappach B, Jan YN, Jan LY (1999) A new ER trafficking signal regulates the subunit stoichiometry of plasma membrane K(ATP) channels. *Neuron* 22:537–548
27. Rauh R, Diakov A, Tzschope A, Korbmacher J, Azad AK, Cuppens H, Cassiman J-J, Dötsch J, Sticht H, Korbmacher C (2010) A mutation of the epithelial sodium channel associated with atypical cystic fibrosis increases channel open probability and reduces Na⁺ self inhibition. *J Physiol* 588:1211–1225
28. McAlear SD, Liu X, Williams JB, McNicholas-Bevensee CM, Bevensee MO (2006) Electrogenic Na/HCO₃ cotransporter (NBCe1) variants expressed in *Xenopus* oocytes: functional comparison and roles of the amino and carboxy termini. *J Gen Physiol* 127:639–658
29. Hille B (2001) Ionic channels of excitable membranes. 3. Sinauer Ass, MA, USA
30. Knütter I, Kottra G, Fischer W, Daniel H, Brandisch M (2009) High-affinity interaction of sartans with H⁺/peptide transporters. *Drug Metab Dispos* 37:143–149
31. Meredith D (2009) The mammalian proton-coupled peptide cotransporter PepT1: sitting on the transporter-channel fence? *Phil Trans R Soc Lond B* 364:203–207
32. Amasheh S, Wenzel U, Boll M, Dorn D, Weber W-M, Claus W, Daniel H (1997) Transport of charged dipeptides by the intestinal H⁺/peptide symporter PepT1 expressed in *Xenopus laevis* oocytes. *J Membr Biol* 155:247–256
33. Kottra G, Stamford A, Daniel H (2002) PEPT1 as a paradigm for membrane carriers that mediate electrogenic bidirectional transport of anionic, cationic, and neutral substrates. *J Biol Chem* 277:32683–32691
34. Sala-Rabanal M, Loo DDF, Hirayama BA, Turk E, Wright EM (2006) Molecular interactions between dipeptides, drugs and the human intestinal H⁺/oligopeptide cotransporter, hPEPT1. *J Physiol* 574:149–166
35. Sangaletti R, Terova G, Peres A, Bossi E, Corà S, Saroglia M (2009) Functional expression of the oligopeptide transporter PepT1 from the sea bass *Dicentrarchus labrax*. *Pflug Arch* 459:47–54
36. Fesce R, Giovannardi S, Binda F, Bossi E, Peres A (2002) The relation between charge movement and transport-associated currents in the GABA cotransporter rGAT1. *J Physiol* 545:739–750
37. Hodgkin AL, Huxley AF (1952) The components of membrane conductance in the giant axon of *Loligo*. *J Physiol* 116:473–496